

Mixed-Valent Diruthenium Long-Chain Carboxylates. 2. Magnetic Properties[†]

Fabio D. Cukiernik,^{*,‡} Dominique Luneau, Jean-Claude Marchon, and Pascale Maldivi*

Département de Recherche Fondamentale sur la Matière Condensée, Service de Chimie Inorganique et Biologique, Laboratoire de Chimie de Coordination, URA CNRS 1194, CEA-Grenoble, 17 Rue des Martyrs, 38054 Grenoble Cedex 9, France

Received October 28, 1997

The magnetic properties of several mixed-valent diruthenium long-chain carboxylates of general formula $\text{Ru}_2(\text{RCO}_2)_4\text{X}$ ($\text{X} = \text{Cl}$, DOS, or RCO_2 , DOS = dodecyl sulfate, and RCO_2 = linear aliphatic carboxylate or dialkoxy- or trialkoxybenzoate) were studied in the temperature range 6–400 K. All of the compounds exhibit a strong zero-field splitting ($D = \text{ca. } 75 \text{ cm}^{-1}$), independent of the nature of the axial anion X or of the equatorial substituent R. In the $\text{X} = \text{RCO}_2$ series an intermolecular antiferromagnetic (AF) interaction $zJ = \text{ca. } -2 \text{ cm}^{-1}$ was found, whereas in the case of an $\text{X} = \text{DOS}$ analogue, this interaction is very weak (-0.2 cm^{-1}). The $\text{X} = \text{Cl}$ series shows three distinct types of interdimer magnetic exchange: very weak, moderate ($|zJ| \approx 2 \text{ cm}^{-1}$), or strong ($|zJ| > 10 \text{ cm}^{-1}$). One representative complex in this series, $\text{Ru}_2(\text{C}_4\text{H}_9\text{CO}_2)_4\text{Cl}$, has been structurally characterized by X-ray crystallography. Crystal data: tetragonal system, space group $I\bar{4}2d$, $a = 14.137(3) \text{ \AA}$, $c = 26.246(5) \text{ \AA}$, and $Z = 8$. Examination of the structures and magnetic behaviors suggests that the AF exchange in this series correlates with the $\text{Ru}-\text{Cl}-\text{Ru}$ intermolecular angle; a qualitative explanation in terms of overlap of magnetic orbitals is proposed. Magnetic susceptibility measurements in the columnar mesophase of the mesomorphic congeners indicate that no significant structural change occurs at the crystal–liquid crystal transition.

Introduction

Mixed-valent diruthenium tetracarboxylates, of general formula $\text{Ru}_2(\text{RCO}_2)_4\text{X}$ where X is an anionic axial ligand, are the subject of considerable current interest for inorganic and materials chemists.^{1–7} This interest stems from their electronic properties, which are unique among the numerous binuclear transition metal tetracarboxylate complexes. They exhibit a

3-fold accidentally degenerate highest occupied molecular orbital (HOMO), which is filled with three unpaired electrons resulting in a quadruplet ($S = 3/2$) ground state,¹ combined with a multiple (order 2.5) ruthenium–ruthenium bond.^{1c} Besides these electronic properties, the long-chain congeners have been shown to exhibit columnar liquid-crystalline properties, when appropriate sets of equatorial carboxylates and axial anions are obtained.² The combination of these electronic properties with the unidimensional organization in the columns, in the mesomorphic state, may find some applications in new inorganic materials.

The description of the electronic structure of these compounds rests mainly on magnetic susceptibility measurements. In earlier work, the effective magnetic moment (μ_{eff}) at room temperature was found in the range 3.8–4.3 μ_{B} .^{1a,3} per dimer, which for a spin-only behavior, corresponds to three unpaired electrons per dimer. This result was satisfactorily explained by Norman et al. on the basis of a SCF-X α calculation of the electronic structure of the $\text{Ru}_2(\text{HCO}_2)_4^+$ dimer.^{1c} The peculiar magnetic behavior of mixed-valent diruthenium carboxylates in a wide temperature range^{4–6} was interpreted as resulting from a large zero-field splitting (ZFS) with an axial splitting value D of the order of 70 cm^{-1} .^{4,5} In particular, the work that we have carried out earlier⁵ on the acetato complex $[\text{Ru}_2(\text{AcO})_4(\text{H}_2\text{O})_2]\text{BPh}_4$ (see ref 7 for abbreviated notations of compounds) has provided information on the electronic structure of the binuclear dimer as an isolated moiety, without any intermolecular interaction. The influence of different axial ligands (neutral or anionic) on the existence and magnitude of interdimer magnetic exchange in mixed-valent ruthenium carboxylates has also been studied.^{5,6,8} On the basis of a rigorous curve-fitting analysis, we have shown⁵ that pyrazine can mediate antiferromagnetic (AF) interdimer interactions in these systems. We have also proposed that the experimental value of the low-temperature limit of the

(8) Cotton, F. A.; Kim, Y.; Ren, T. *Polyhedron* 1993, 12, 607.

[†] Part 1: see ref 2b.

[‡] Current address: INQUIMAE, Departamento de Química Inorgánica, Analítica y Química Física, Facultad de Ciencias Exactas y Naturales, Universidad de Buenos Aires, Pabellón II, Ciudad Universitaria, Nuñez (1428) Capital Federal, Argentina.

- (1) (a) Stephenson, T. A.; Wilkinson, G. J. *J. Inorg. Nucl. Chem.* 1966, 8, 2285. (b) Bennett, M. J.; Caulton, K. G.; Cotton, F. A. *Inorg. Chem.* 1969, 8, 1. (c) Norman, J. G.; Renzoni, G. E.; Case, D. A. *J. Am. Chem. Soc.* 1979, 101, 5256.
- (2) (a) Cukiernik, F. D.; Maldivi, P.; Giroud-Godquin, A. M.; Marchon, J. C.; Ibn-Elhaj, M.; Guillon, D.; Skoulios, A. *Liq. Cryst.* 1991, 9, 903. (b) Cukiernik, F. D.; Ibn-Elhaj, M.; Chaia, Z. D.; Marchon, J. C.; Giroud-Godquin, A. M.; Guillon, D.; Skoulios, A.; Maldivi, P. *Chem. Mater.* 1998, 10, 83.
- (3) (a) Mukaida, M.; Nomura, T.; Ishimori, T. *Bull. Chem. Soc. Jpn.* 1972, 45, 2143. (b) Das, B. K.; Chakravarty, A. R. *Polyhedron* 1988, 7, 685. (c) Barral, M. C.; Jiménez-Aparicio, R.; Rial, C.; Royer, E.; Saucedo, M. J.; Urbanos, F. A. *Polyhedron* 1990, 9, 1723. (d) Higgins, P.; McCann, M. J. *Chem. Soc., Dalton Trans.* 1988, 661. (e) Carvill, A.; Higgins, P.; McCann, M.; Ryan, H.; Shiels, A. *J. Chem. Soc., Dalton Trans.* 1989, 2435.
- (4) (a) Telsler, J.; Drago, R. S. *Inorg. Chem.* 1984, 23, 3114. (b) Telsler, J.; Miskowsky, V. M.; Drago, R. S.; Wong, N. M. *Inorg. Chem.* 1985, 24, 4765.
- (5) Cukiernik, F. D.; Giroud-Godquin, A. M.; Maldivi, P.; Marchon, J. C. *Inorg. Chim. Acta* 1994, 215, 203.
- (6) (a) Cotton, F. A.; Kim, Y.; Ren, T. *Inorg. Chem.* 1992, 31, 2608. (b) Cotton, F. A.; Kim, Y.; Ren, T. *Inorg. Chem.* 1992, 31, 2723.
- (7) Abbreviations used in this work: BPh_4 = tetraphenylborate; AcO = acetate; prop = propionate; but = butyrate; DOS = dodecyl sulfate; B2OCn = 3,4-di-*n*-alkoxybenzoate where the alkoxy chain is linear, saturated and possesses *n* carbon atoms; B3OCn = 3,4,5-tri-*n*-alkoxybenzoate.

effective magnetic moment provides an easy criterion of intermolecular exchange in these highly zero-field-split systems.

We have now extended our magnetic studies to a wide number of mixed-valent diruthenium long-chain carboxylates, which are also of interest for their liquid-crystalline properties: $\text{Ru}_2(\text{O}_2\text{C}-(\text{CH}_2)_{n-2}-\text{CH}_3)_5$ for $n = 6, 8, 9, 12, 14,$ or 16 ; $\text{Ru}_2(\text{O}_2\text{C}-(\text{CH}_2)_{14}-\text{CH}_3)_4\text{DOS}$; $\text{Ru}_2(\text{O}_2\text{C}-(\text{CH}_2)_{n-2}-\text{CH}_3)_4\text{Cl}$ for $n = 2, 3, 4, 5, 8,$ or 9 ; $\text{Ru}_2(\text{BmOCn})_4\text{Cl}^7$ with $m = 2, n = 12$ or 16 (disubstituted benzoate) and $m = 3, n = 1$ (trisubstituted benzoate). We have investigated in special detail the influence of the equatorial carboxylate and of the anion on the magnitude of the ZFS parameter D , and we have focused our attention on the possible intermolecular interactions mediated by different anions acting as axial ligands. As it was necessary to get new structural information to rationalize the magnetic behavior of the chloro complexes $\text{Ru}_2(\text{RCO}_2)_4\text{Cl}$, we have solved the crystal structure of the short-chain congener $\text{Ru}_2(\text{O}_2\text{C}-(\text{CH}_2)_3-\text{CH}_3)_4\text{Cl}$. Finally, we have used molecular magnetic measurements as a local probe to gain structural information about the coordination environment of Ru in the liquid-crystalline phase by examining the magnetic behavior throughout the phase transition of these metallomesogens.

Experimental Section

Synthesis and Characterization. The synthesis and purification of the $\text{Ru}_2(\text{O}_2\text{C}-(\text{CH}_2)_{n-2}-\text{CH}_3)_5$; $\text{Ru}_2(\text{O}_2\text{C}-(\text{CH}_2)_{n-2}-\text{CH}_3)_4\text{DOS}$; $\text{Ru}_2(\text{O}_2\text{C}-(\text{CH}_2)_{n-2}-\text{CH}_3)_4\text{Cl}$; and $\text{Ru}_2(\text{B2OCn})_4\text{Cl}$ series have been described elsewhere.^{2b}

$\text{Ru}_2(\text{B3OC1})_4\text{Cl}$. This complex was obtained by room-temperature reaction of 600 mg (1.02 mmol) of $\text{Ru}_2(\text{but})_4\text{Cl}$ with 3.50 g (16 mmol) of 3,4,5-tri(methoxy)benzoic acid in 150 mL of methanol. The precipitate which appeared after 2 days was filtered off, washed with methanol, and then dried under vacuum.

All of the complexes were characterized by UV/vis and IR spectroscopies, elemental analysis of C, H, Ru, Cl, and S (when present). See ref 2 for details on the syntheses and characterizations. The elemental analyses are provided in the Supporting Information.

Structure Determination. Single crystals of $\text{Ru}_2(\text{O}_2\text{C}-(\text{CH}_2)_3-\text{CH}_3)_4\text{Cl}$ were obtained by overnight cooling of a saturated solution (at 60 °C) of the complex in pentanoic acid. Chlorotetrakis(*n*-pentanoato)-diruthenium(II,III) crystallizes in the tetragonal system as dark-red needles. A crystal of dimensions $0.15 \times 0.15 \times 0.50 \text{ mm}^3$ was used for the collection of the diffracted intensities on a four-circle CAD4 Enraf-Nonius diffractometer, equipped with a graphite monochromator for Mo K α ($\lambda = 0.7107 \text{ \AA}$) radiation in the $\omega-2\theta$ mode at room temperature. Lattice parameters were refined by least-squares methods, using 25 reflections ($10^\circ \leq \theta \leq 15^\circ$) chosen for their regular spatial spreading. During the collection, three test *hkl* reflections were measured every 2 h and did not show any decay in intensity. The orientation of the crystal was checked every 250 reflections by centering the test reflections. After Lorentz and polarization factors correction, 2183 reflections ($I > 4\sigma$) were used for the structure determination. No absorption correction was performed. The crystallographic data are summarized in Table 1. The observation of systematic extinctions *hkl* following $h + k + l = 2n$ and $2h + l = 4n$ is compatible with two space groups: $I\bar{4}2d$ and $I4_1md$. Examination of the Patterson function led us to select the former. The positions of the ruthenium ion and of its coordination sphere atoms (Cl, O) were determined by the heavy-atom method, using SHELX86,⁹ and then entered in the refinement process using SHELX76,¹⁰ with the chloride ion on special position *d* with an occupancy factor of $1/2$. The atomic diffusion factors used

Table 1. Crystallographic Data for $\text{Ru}_2(\text{C}_5\text{H}_9\text{O}_2)_4\text{Cl}$

formula	$\text{Ru}_2\text{C}_{20}\text{H}_{36}\text{O}_8\text{Cl}$
fw	642.08
<i>T</i> (K)	293
space group	$I\bar{4}2d$
<i>Z</i>	8
<i>a</i> (Å)	14.137(3)
<i>c</i> (Å)	26.246(5)
<i>V</i> (Å ³)	5246 (2)
<i>D_c</i> (g cm ⁻³)	1.627
μ (Mo K α) (cm ⁻¹)	12.24
<i>R^a</i>	0.0272
<i>R_w^b</i>	0.0294

$$^a R = \sum ||F_o| - |F_c|| / \sum |F_o|. \quad ^b R_w = \sum w(|F_o| - |F_c|)^2 / \sum w|F_o|^2)^{1/2}.$$

Table 2. Atomic Coordinates ($\times 10^4$) and Equivalent Isotropic Displacement Parameters

atom	<i>x</i>	<i>y</i>	<i>z</i>	<i>U_{eq}^a</i> (Å ²)
Ru	0.97664(2)	0.42243(2)	0.12513(2)	0.0346(2)
Cl	0.9179(1)	0.250	0.1250	0.0471(4)
O1	0.9252(4)	0.6055(3)	0.1789(2)	0.043(1)
O2	0.8798(3)	0.4533(3)	0.1791(2)	0.043(1)
O3	0.9262(4)	0.6051(3)	0.0703(2)	0.048(1)
O4	0.8809(4)	0.4542(3)	0.0700(2)	0.048(1)
C1	0.8705(5)	0.5393(4)	0.1941(2)	0.037(1)
C2	0.8754(6)	0.5378(5)	0.0533(3)	0.050(2)
C3	0.7915(6)	0.5607(6)	0.2302(3)	0.052(2)
C4	0.8078(8)	0.5605(6)	0.0120(4)	0.086(3)
C5	0.7004(7)	0.565(1)	0.2034(4)	0.126(6)
C6	0.780(1)	0.6554(7)	0.0051(5)	0.120(5)
C7	0.680(1)	0.596(2)	0.1591(6)	0.23(2)
C8	0.716(1)	0.681(1)	-0.0374(7)	0.180(9)
C9	0.5924(9)	0.607(1)	0.1310(8)	0.134(5)
C10	0.656(2)	0.634(1)	-0.0577(9)	0.28(2)

^a *U_{eq}* is defined as one-third of the orthogonalized *U_{ij}* tensor.

were those proposed by Cromer and Waber,¹¹ corrected for anomalous dispersion effects.¹² Other atoms, with the exception of hydrogen atoms, were localized by successive difference Fourier synthesis and least-squares refinement. Atomic positions and thermal parameters are presented in Table 2. The carbon atoms belonging to the pentyl groups showed significant thermal motion at the chain ends, resulting in a low accuracy in carbon-carbon interatomic distances. The use of several models of disorder did not improve the results. We have therefore included the influence of this thermal disorder for the calculation of interatomic distances between these atoms, by taking into account both the position of their thermal vibration ellipsoids and their relative displacements. The distances thus obtained were slightly greater than those expected, confirming the strong influence of the thermal disorder. The absolute structure configuration was determined by calculation of the Flack's parameter.¹³ Hydrogen atoms were placed on calculated positions at a distance of 1.08 Å from the corresponding carbon atoms; their thermal vibration parameters were maintained fixed and isotropic. It should be noted that the difference Fourier synthesis values obtained after the last refinement show the presence of a weak residual electronic density between the two ruthenium ions (Table 1). The final refinement cycle gave reliability factor values of $R = 0.0272$ and $R_w = 0.0294$. The collection conditions and crystallographic data, the calculated positions of hydrogen atoms, the complete listing of bond lengths and bond angles and anisotropic parameters are deposited as Supporting Information.

Magnetic Measurements. The magnetic susceptibility measurements between 6 and 400 K were performed on Quantum Design MPMS or SHE VTS905 SQUID susceptometers in a magnetic field of

- (9) Sheldrick, G. M. In *Crystallographic Computing 3*; Sheldrick, G. M., Krüger, C., Goddard, R., Eds.; Oxford University Press: England, 1985; pp 175-179.
 (10) Sheldrick, G. M. *SHELX 76: Program for Crystal Structure Determination*; University of Cambridge: England, 1976.

- (11) Cromer, D. T.; Waber, J. T. In *International Tables for X-ray Crystallography*; Ibers, J. A., Hamilton, W. C., Eds.; Kynoch Press: Birmingham, England, 1974; Vol. IV, Table 2.2B, pp 99-101.
 (12) Cromer, D. T. In *International Table for X-ray Crystallography*; Ibers, J. A., Hamilton, W. C., Eds.; Kynoch Press: Birmingham, England, 1974; Vol. IV, Table 2.3.1, p 149.
 (13) Flack, H. D. *Acta Crystallogr.* **1985**, *A41*, 500.

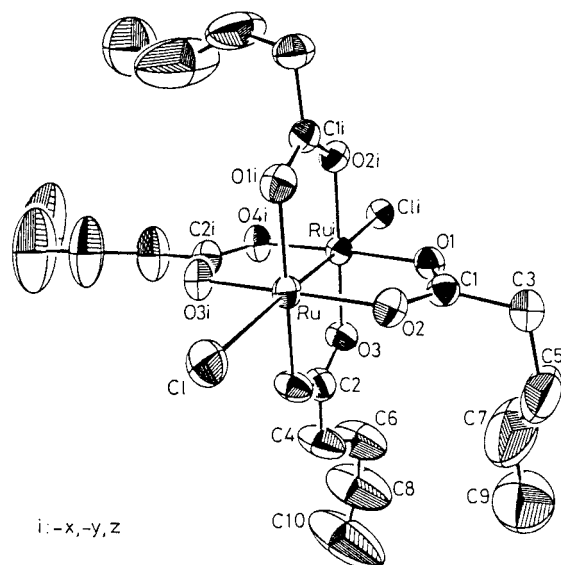


Figure 1. ORTEP representation of the binuclear unit of $\text{Ru}_2(\text{O}_2\text{C}-\text{C}_4\text{H}_9)_4\text{Cl}$.

5000 G. The powdered samples, typically 20–60 mg, were placed in a small (5-mm diameter) plastic pan. Raw magnetic data were corrected for the contribution of the sample holder and for the diamagnetism of the complexes, evaluated by using Pascal's constants.¹⁴ Higher temperatures (up to 550 K), for the liquid-crystalline phase of $\text{Ru}_2(\text{RCO}_2)_5$ compounds, were obtained with the oven designed for the QD MPMS system. In these cases, the use of a very small (2-mm diameter) aluminum sample holder, containing typically 1.5–6 mg of product, was necessary. The compounds measured with this oven/sample holder configuration in the high-temperature range (350–550 K) were subjected first to two independent measurement cycles for the low (6–400 K) temperature range: the first one using the same aluminum micro-container, the second one using the usual plastic container. The two sets of magnetic data were identical after correction of the various contributions described above. The molar magnetic susceptibility data thus obtained were refined with theoretical analytical expressions by a least-squares procedure, using a locally developed Fortran program (written by Dr. P. H. Fries, CEA-Grenoble, France).

Results

Crystal and Molecular Structure of $\text{Ru}_2[\text{O}_2\text{C}-(\text{CH}_2)_3-\text{CH}_3]_4\text{Cl}$. The unit cell contains eight diruthenium units. As can be seen in Figure 1, which shows the ORTEP^{14,15} representation of one binuclear unit, the molecular structure is similar to that found earlier for other members of this series.^{1b,3,6,8,16,17} The two ruthenium atoms are equatorially linked by the four bridging carboxylates, and the chloride anion is axially coordinated. Selected interatomic distances and angles are reported in Table 3 (the effect of the thermal motion on the terminal carbon–carbon interatomic distances has already been discussed in the Experimental Section). The Ru–Ru, Ru–Cl, and

Table 3. Bond Lengths (Å) and Angles (deg)

Ru–Ru ^a	2.2899(8)	C1–C3	1.500(7)	
Ru–Cl	2.5774(9)	C2–C4	1.476(9)	
Ru–O1 ^a	2.018(3)	C3–C5	1.475(9)	
Ru–O2	2.020(4)	C4–C6	1.41(1)	1.59(1) ^c
Ru–O3 ^a	2.026(3)	C5–C7	1.31(2)	1.62(2) ^c
Ru–O4	2.031(4)	C6–C8	1.47(2)	1.53(2) ^c
O1–C1	1.282(6)	C7–C9	1.41(1)	1.51(2) ^c
O2–C1	1.279(5)	C8–C10	1.20(2)	1.69(2) ^c
O3–C2	1.270(6)			
O4–C2	1.267(6)			
Ru ^a –Ru–Cl	177.94(4)	O3 ^a –Ru–O4	89.2(2)	
Ru ^a –Ru–O1 ^a	89.4(1)	Ru–Cl–Ru ^b	142.3(1)	
Ru ^a –Ru–O2	89.4(1)	O1–C1–O2	122.5(5)	
Ru ^a –Ru–O3 ^a	89.3(1)	O1–C1–C3	119.8(4)	
Ru ^a –Ru–O4	89.0(1)	O2–C1–C3	117.6(5)	
Cl–Ru–O1 ^a	92.1(1)	O3–C2–O4	122.8(5)	
Cl–Ru–O2	89.2(1)	O3–C2–C4	118.1(5)	
Cl–Ru–O3 ^a	92.1(1)	O4–C2–C4	119.2(5)	
Cl–Ru–O4	89.5(1)	C1–C3–C5	110.9(5)	
O1 ^a –Ru–O2	90.9(2)	C2–C4–C6	118.4(7)	
O1 ^a –Ru–O3 ^a	89.6(1)	C3–C5–C7	131.1(8)	
O1 ^a –Ru–O4	178.0(1)	C4–C6–C8	120.0(8)	
O2–Ru–O3 ^a	178.5(1)	C5–C7–C9	134(1)	
O2–Ru–O4	90.2(2)	C6–C8–C10	130(1)	

^a –x, –y, z. ^b x, –y + 1/2, z + 1/4. ^c Interatomic distance averaged over thermal motion (see text).

equatorial Ru–O distances agree with the values already published for all other mixed-valent diruthenium carboxylates. Two adjacent aliphatic chains exhibit a gauche conformation at the first methylene group, whereas the other aliphatic chains adopt a zigzag trans conformation up to the fourth carbon atom and then a gauche conformation at the C(8)–C(10) bond.

In the crystal lattice, the binuclear entities are bridged by the chloride ions, giving infinite "...–complex–anion–complex–anion–..." zigzag "chains" packed along the *c* direction, the propagation direction of these chains being parallel alternatively to the *a* and *b* axes. The general features of the supramolecular structure closely resemble those reported for the $I42d$ form of the butyrate analogue.^{1b} The main difference between the two complexes lies in the value of the Ru–Cl–Ru angle: 142.3° in the present case vs 125° for the former.

Magnetic Susceptibility Studies. All the complexes studied in this work exhibited χT values between 2.1 and 2.3 cm³ K/mol at room temperature ($\mu_{\text{eff}} \approx 4.1\text{--}4.3 \mu_{\text{B}}$), consistent with the presence of three unpaired electrons. At low temperatures the χT curves fall down, and this fall may be attributed primarily to the ZFS.^{4,6} The equations describing the temperature dependence of the molar magnetic susceptibility of a quadruplet state undergoing an axial ZFS are^{4b,18}

$$\chi_{\parallel} = \frac{Ng^2\beta^2}{kT} \frac{1 + 9e^{-2D/kT}}{4(1 + e^{-2D/kT})} \quad (1)$$

$$\chi_{\perp} = \frac{Ng^2\beta^2}{kT} \frac{4 + (3kT/D)(1 - e^{-2D/kT})}{4(1 + e^{-2D/kT})} \quad (2)$$

(14) Selwood, P. W. *Magnetochemistry*, 2nd ed.; Interscience: New York, 1956; p 78.

(15) (a) Johnson, C. K. ORTEP, Report ORNL-3794; Oak Ridge National Laboratory: Oak Ridge, TN, 1965. (b) Michalowicz, D. A.; Michalowicz, A. MACORTEP; Laboratoire de Physicochimie Structurale, Université Paris Val de Marne, UFR de Sciences et Technologies, 94010 Créteil.

(16) (a) Lindsay, A. J.; Wilkinson, G.; Motevalli, M.; Hursthouse, M. B. *J. Chem. Soc., Dalton Trans.* **1987**, 2723. (b) Togano, T.; Mukaida, M.; Nomura, T. *Bull. Chem. Soc. Jpn.* **1980**, *53*, 2085. (c) Bino, A.; Cotton, F. A.; Felthouse, T. R. *Inorg. Chem.* **1979**, *18*, 2599. (d) Marsh, R. E.; Schomaker, V. *Inorg. Chem.* **1981**, *20*, 299. (e) Kimura, T.; Sakurai, T.; Shima, M.; Togano, T.; Mukaida, M.; Nomura, T. *Bull. Chem. Soc. Jpn.* **1982**, *55*, 3927. (f) Miskowsky, V. M.; Loher, T. M.; Gray, H. B. *Inorg. Chem.* **1987**, *26*, 1098.

(17) (a) McCann, G. M.; Carvill, A.; Guinan, P.; Higgins, P.; Campbell, J.; Ryan, H.; Walsh, M.; Ferguson, G.; Gallagher, J. *Polyhedron* **1991**, *10*, 2273. (b) Das, B. K.; Chakravarty, A. R. *Polyhedron* **1991**, *10*, 491. (c) Barral, M. C.; Jiménez-Aparicio, R.; Priego, J. L.; Royer, E. C.; Gutiérrez-Puebla, E.; Ruiz Valero, C. *Polyhedron* **1992**, *11*, 2209. (d) Martin, D. S.; Newman, R. A.; Vlasnik, L. S. *Inorg. Chem.* **1980**, *26*, 3404. (e) McCann, M.; Carvill, A.; Cardin, C.; Convery, M. *Polyhedron* **1993**, *12*, 1163. (f) Cotton, F. A.; Matusz, M.; Zhong, B. *Inorg. Chem.* **1988**, *27*, 4368. (g) Spohn, M.; Strähle, J.; Hiller, W. Z. *Naturforsch.* **1986**, *41B*, 541.

The average molar magnetic susceptibility of a powdered sample is given by

$$\chi = \frac{1}{3}(\chi_{\parallel} + 2\chi_{\perp}) + \text{TIP} \quad (3)$$

where TIP is the temperature independent paramagnetism.

In some cases, it was necessary to include the contribution of an impurity present in a proportion P and which was assumed to follow a Curie law with $S = 1/2$ and a g factor noted as g_{mo} . This means that the quality of the fits was significantly improved when taking into account this contribution. The complete expression of the magnetic susceptibility used for the refinements was therefore

$$\chi_{\text{mol}} = (1 - P)\chi + P \frac{N\beta^2 g_{\text{mo}}^2}{4kT} \quad (4)$$

The systems for which χT vs T behavior was satisfactorily refined with this model (eqs 1–4) will be noted $\{^{3/2}, \text{ZFS}\}$ below.

However, for some of the compounds, the fall in the curve χT vs T at low temperatures was too pronounced to be ascribed only to a ZFS, and some kind of intermolecular AF interaction had to be considered. The examination of the low temperature behavior of χ was useful to detect the presence of these interdimer interactions (see ref 5 for a detailed discussion). In most cases, the AF interaction was weak, as there was no maximum above 6 K in the $\chi(T)$ curve. Consequently, the molecular field approximation (MFA) may be used with the following analytical expression¹⁸

$$\chi' = \frac{\chi}{1 - (2zJ/Ng^2\beta^2)\chi} \quad (5)$$

where zJ is the exchange energy J multiplied by the number z of interacting neighbors, and χ is the magnetic susceptibility of an isolated molecule, resulting from eq 3. This model will be referred hereafter as the $\{^{3/2}, \text{ZFS}, \text{MFA}\}$ model. As above, the contribution of a paramagnetic impurity was included to yield the complete expression used for the refinements

$$\chi_{\text{mol}} = (1 - P)\chi' + P \frac{N\beta^2 g_{\text{mo}}^2}{4kT} \quad (6)$$

Ru₂(O₂C–(CH₂)_{*n*–2}–CH₃)₅ Series. Figure 2 shows the molar magnetic susceptibility χ and the product χT as a function of temperature for the $n = 16$ compound. Similar results were obtained for the compounds with $n = 6, 8, 9, 12,$ and 14 . At low temperature, χT clearly falls below the zero-temperature limit predicted by the analytical law corresponding to the $\{^{3/2}, \text{ZFS}\}$ model. This observation combined with the absence of a maximum in the χ vs T curve, led us to refine the experimental data with eq 6, corresponding to the $\{^{3/2}, \text{ZFS}, \text{MFA}\}$ model. This was achieved by adjusting the following parameters: $P, g_{\text{mo}}, g_{\parallel}, g_{\perp}, D, zJ,$ and TIP , and a very good agreement was obtained between experimental and calculated curves, as can be seen in Figure 2. Table 4 contains the values of the magnetic parameters ($P, g_{\parallel}, g_{\perp}, \text{TIP}, D,$ and zJ) obtained in the best fits, together with σ^2 , which indicates the quality of the fits. During the refinement process, we have observed that some parameters were correlated (g and TIP , or g and D), leading to the fact that many sets of slightly different parameters gave reasonable fits. On this basis, we have estimated the uncertainty on D as 10

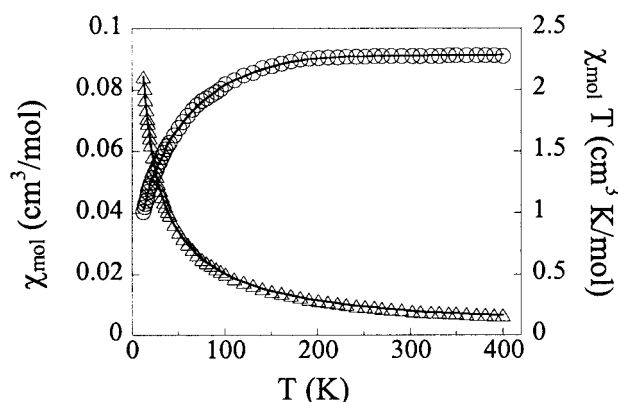


Figure 2. Temperature dependence of the molar magnetic susceptibility χ (Δ) and the product χT (\circ) for complex $\text{Ru}_2(\text{O}_2\text{C}-(\text{CH}_2)_{14}-\text{CH}_3)_5$. Solid lines correspond to the values calculated with the model described in the text; the dashed line corresponds to the zero-temperature limit of χT , calculated as in ref 5.

cm^{-1} and on g as 0.07, the quality of the refinements being much more sensitive to the zJ value.

The values of the magnetic parameters g (in the range 2–2.4) and D (in the range 60–94 cm^{-1}) obtained for the complexes belonging to this series are similar to those reported previously for “noninteracting” mixed-valent diruthenium tetracarboxylates.^{4,5} The g_{\perp} and g_{\parallel} values are higher than 2.0, and in addition, $g_{\parallel} < g_{\perp}$, as in the case of the $[\text{Ru}_2(\text{AcO})_4(\text{H}_2\text{O})_2]\text{BPh}_4$ ⁵ complex, which contains isolated dimers. The D value is close to 70 cm^{-1} , in good agreement with values published for $[\text{Ru}_2(\text{AcO})_4(\text{H}_2\text{O})_2]\text{BPh}_4$ (72 cm^{-1})⁵ and $\text{Ru}_2(\text{but})_4\text{Cl}$ (71 cm^{-1}).⁴ The TIP values found in this series are negligible. The value found for the exchange parameter zJ , ca. -2 cm^{-1} , points to a weak AF interdimer interaction. It is reasonable to assume that intermolecular exchange is mediated by the anionic carboxylate, and that, in the entire series studied here, this anion is μ -1,3 bridging neighboring dimers, as in the case of the propionate^{17f} and benzoate^{17g} analogues. In those cases, the crystalline structure shows the existence of “chains” of alternating ... – complex – anion – ... which are parallel one to each other.

Ru₂(O₂C–(CH₂)₁₄–CH₃)₄DOS. At low temperature, the experimental values of χT are close to the theoretical limit of the $\{^{3/2}, \text{ZFS}\}$ law, and only a very weak AF interaction (i.e., zJ parameter) is needed to obtain a good refinement. The values of the magnetic parameters obtained in the best fit, using eq 6, i.e., the $\{^{3/2}, \text{ZFS}, \text{MFA}\}$ model, are included in Table 4.

Ru₂(RCO₂)₄Cl Series. The chloride series exhibit the same general trends as $[\text{Ru}_2(\text{AcO})_4(\text{H}_2\text{O})_2]\text{BPh}_4$, $\text{Ru}_2(\text{O}_2\text{C}-(\text{CH}_2)_{14}-\text{CH}_3)_4\text{DOS}$ and the $\text{Ru}_2(\text{O}_2\text{C}-(\text{CH}_2)_{n-2}-\text{CH}_3)_5$ series, i.e., a $S = 3/2$ ground-state undergoing a large ZFS, with D values in the range 60–80 cm^{-1} . The differences among the members of the present series arise from the magnitude of the interdimer coupling. In that sense, we have identified three types of behavior: The first one (type I) corresponds to inexistent or extremely weak intermolecular AF interactions. The experimental $\chi(T)$ and $\chi T(T)$ curves are similar to those obtained for the complex $[\text{Ru}_2(\text{AcO})_4(\text{H}_2\text{O})_2]\text{BPh}_4$ ⁵ and the $\{^{3/2}, \text{ZFS}\}$ model applies well. This behavior has been observed for the acetate $\text{Ru}_2(\text{AcO})_4\text{Cl}$ and the 3,4,5-trimethoxybenzoate $\text{Ru}_2(\text{B3OC1})_4\text{Cl}$, as well as for the butyrate complex $\text{Ru}_2(\text{but})_4\text{Cl}$, that we have reexamined as a starting point and which gave the same magnetic data as those reported by Drago et al.⁴ In the case of the acetate derivative, however, a very weak intermolecular interaction does improve the refinement. The values of the magnetic parameters obtained in the best refinements are reported in Table 5.

(18) O'Connor, C. J. *Prog. Inorg. Chem.* **1982**, 29, 203.

Table 4. Magnetic Parameters and Goodness-of-Fit Obtained by Nonlinear Fitting for Mixed-Valent Diruthenium Carboxylates Possessing Long-Chain Anions as Axial Ligands (D and zJ in cm^{-1} , TIP in cm^3/mol , P in %, $\sigma^2 = (\sum(\chi_{\text{calc}} - \chi_{\text{exp}})^2)/\sum\chi_{\text{exp}}^2$)

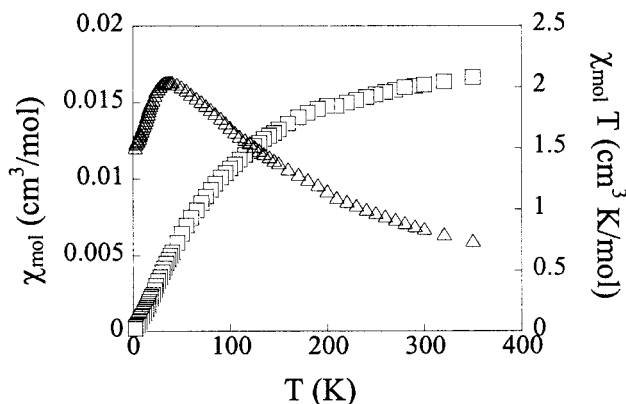
compd	P	g_{\parallel}	g_{\perp}	TIP	D	zJ	σ^2
$\text{Ru}_2(\text{O}_2\text{C}-(\text{CH}_2)_{n-2}-\text{CH}_3)_5$							
$n = 6$	0.01	2.09	2.40	1×10^{-5}	60	-3.1	4.6×10^{-5}
$n = 8$	1.2	2.01	2.29	$< 1 \times 10^{-7}$	78	-1.5	2.1×10^{-5}
$n = 9$	0.20		2.32 ^a	7×10^{-7}	70	-3.2	2.6×10^{-4}
$n = 12$	0.08	2.06	2.27	1×10^{-6}	72	-1.7	2.1×10^{-5}
$n = 14$	0.3		2.33 ^a	5.5×10^{-6}	94	-2.4	3.4×10^{-5}
$n = 16$	0.8	2.02	2.29	1×10^{-7}	71	-1.7	1.1×10^{-5}
$\text{Ru}_2(\text{O}_2\text{C}-\text{C}_{15}\text{H}_{31})_4\text{DOS}$							
$n = 16$	0.18	2.17	2.19	1×10^{-6}	72	-0.21	2.1×10^{-6}

^a Calculated using only one isotropic $g = g_{\parallel} = g_{\perp}$ factor.

Table 5. Magnetic Parameters and Goodness-of-Fit Obtained by Nonlinear Fitting for Mixed-Valent Diruthenium Carboxylates Possessing a Chloride Anion as Axial Ligand (D and zJ in cm^{-1} , TIP in cm^3/mol , P in %, $\sigma^2 = (\sum(\chi_{\text{calc}} - \chi_{\text{exp}})^2)/\sum\chi_{\text{exp}}^2$)

compd	P	g_{\parallel}	g_{\perp}	TIP	D	zJ	σ^2
$\text{Ru}_2(\text{but})_4\text{Cl}$	0.30	2.14	2.25	$< 1 \times 10^{-6}$	69		8.3×10^{-5}
$\text{Ru}_2(\text{AcO})_4\text{Cl}^a$	0.03	2.12	2.20	2.8×10^{-5}	75	-0.19	4.6×10^{-6}
$\text{Ru}_2(\text{B3OC1})_4\text{Cl}$	2.60	2.25	2.22	5×10^{-5}	64	0.00	2.4×10^{-5}
$\text{Ru}_2(\text{O}_2\text{C}-\text{C}_4\text{H}_9)_4\text{Cl}$	0.16	2.01	2.17	2.3×10^{-4}	67	-4.6	1.9×10^{-4}
$\text{Ru}_2(\text{O}_2\text{C}-\text{C}_7\text{H}_{15})_4\text{Cl}$	0.26	2.01	2.26	3×10^{-6}	80	-0.9	1.4×10^{-5}
$\text{Ru}_2(\text{O}_2\text{C}-\text{C}_8\text{H}_{17})_4\text{Cl}$	0.90	2.23	2.27	5×10^{-5}	75	-0.9	4.6×10^{-5}
$\text{Ru}_2(\text{B2OC12})_4\text{Cl}$	0.02		2.12 ^b	4.5×10^{-4}	73	-2.4	3.2×10^{-5}
$\text{Ru}_2(\text{B2OC16})_4\text{Cl}$	0.01		2.29 ^b	5.8×10^{-4}	76	-3.2	2.9×10^{-6}

^a A refinement performed by fixing the exchange parameter to zero gave the following parameters: $P = 1.16$, $g_{\parallel} = 1.97$, $g_{\perp} = 2.12$, TIP = 6.8×10^{-4} , $D = 54$, $\sigma^2 = 7 \times 10^{-5}$. ^b Calculated using only one isotropic g factor.

**Figure 3.** Plots of molar magnetic susceptibility χ (Δ) and product χT (\square) as a function of temperature for the complex $\text{Ru}_2(\text{O}_2\text{C}-\text{CH}_2\text{CH}_3)_4\text{Cl}$.

The second kind of behavior (type II) that was observed corresponds to experimental $\chi(T)$ and $\chi T(T)$ curves similar to those obtained for $\text{Ru}_2(\text{RCO}_2)_5$ compounds. The complexes belonging to this family were linear aliphatic carboxylates with $n = 5, 8, \text{ or } 9$ and the two long-chain alkoxybenzoate derivatives $\text{Ru}_2(\text{B2OC12})_4\text{Cl}$ and $\text{Ru}_2(\text{B2OC16})_4\text{Cl}$. The experimental curves were refined with the $\{^{3/2}, \text{ZFS}, \text{MFA}\}$ model. Not surprisingly, the zJ values (ca. -1 to -5 cm^{-1}) obtained by least-squares refinements were similar to those found for $\text{Ru}_2(\text{RCO}_2)_5$ (see values in Table 5).

A third magnetic behavior was identified, for the chloro-propionate derivative. A pronounced decrease of the curve of $\chi T(T)$ at the zero-temperature limit is observed (See Figure 3), which points to a stronger AF interaction than those observed for type II complexes. This behavior is more clearly seen in the curve of $\chi(T)$, which exhibits a maximum at ca. 35 K, as shown in Figure 3. A similar experimental behavior has recently been found for the complex $\text{Ru}_2(\text{Ph}_2\text{CCH}_3\text{CO}_2)_4\text{Cl}$,⁸ although the published experimental curve revealed the presence of some paramagnetic impurity.

The molecular field approximation is valid only for weak magnetic interactions, and its mathematical expression does not predict a maximum in the $\chi(T)$ curve, it was thus not adequate for this kind of magnetic behavior. In fact, a model describing a unidimensional chain of strongly interacting $S = 3/2$ units with a high ZFS leads to a high degree of mathematical complexity, and no analytical solution has yet been published. Therefore it has not been possible to perform a reliable refinement for this complex.¹⁹ The maximum in $\chi(T)$ at 35 K allows us to state that the AF exchange between neighbors is certainly greater (in absolute value) than 10 cm^{-1} .

Magnetic Behavior at the Crystal-Liquid Crystal Phase Transition. The evolution of the magnetic susceptibility through the crystal-to-columnar mesophase transition was examined for several complexes, to get some insight into the local environment of the metallic centers during this transition. No discontinuity in the magnetic susceptibility curve was found at the transition temperature, for all the complexes studied: $\text{Ru}_2(\text{RCO}_2)_5$ for $n = 12, 14, \text{ and } 16$ (transition at ca. $150 \text{ }^\circ\text{C}$)², $\text{Ru}_2(\text{B2OC16})_5$ (transition at ca. $45 \text{ }^\circ\text{C}$),^{2b} $\text{Ru}_2(\text{B2OC12})_4\text{Cl}$ (transition at $145 \text{ }^\circ\text{C}$),^{2b} and $\text{Ru}_2(\text{O}_2\text{C}-(\text{CH}_2)_{14}-\text{CH}_3)_4\text{DOS}$ (transition at $142 \text{ }^\circ\text{C}$).^{2b}

Discussion

Interpretation of the Magnetic Behavior of the $\text{Ru}_2(\text{RCO}_2)_4\text{Cl}$ Series. Independently of the type of behavior (type I or II), the main magnetic parameters (g and D) given by the refinement procedure were the same for all the chloro complexes and similar to those obtained for the pentacarboxylate analogues. This result shows that they are intrinsically related to the structure and nature of the binuclear core, with a negligible influence of the axial ligand.

Three types of interdimer exchange have been experimentally observed among this chloro-carboxylato series. In the case of

(19) A similar case with a simpler model, i.e., without ZFS, and assuming infinite chains of interacting $S = 3/2$ spin centers has been described,⁸ but neglect of the ZFS is certainly a rough approximation in such systems, where there is enough evidence that a high value of ZFS (ca. 70 cm^{-1}) is always present.

Table 6. Correlation between Type of Magnetic Behavior and Interdimer Angle Ru–Cl–Ru in the Chloro Complex Series

compd	type of magnetic behavior ^a	Ru–Cl–Ru angle (deg)	ref of the structure
Ru ₂ (AcO) ₄ Cl	I	127.6	16b
Ru ₂ (but) ₄ Cl	I	125.4	1b
Ru ₂ (O ₂ C–C ₄ H ₉) ₄ Cl	II	143.2	this work
Ru ₂ (prop) ₄ Cl	III	180	16c,d
Ru ₂ (Ph ₂ (CH ₃)CCO ₂) ₄ Cl	III ^b	180	8

^a See text. ^b Reference 8.

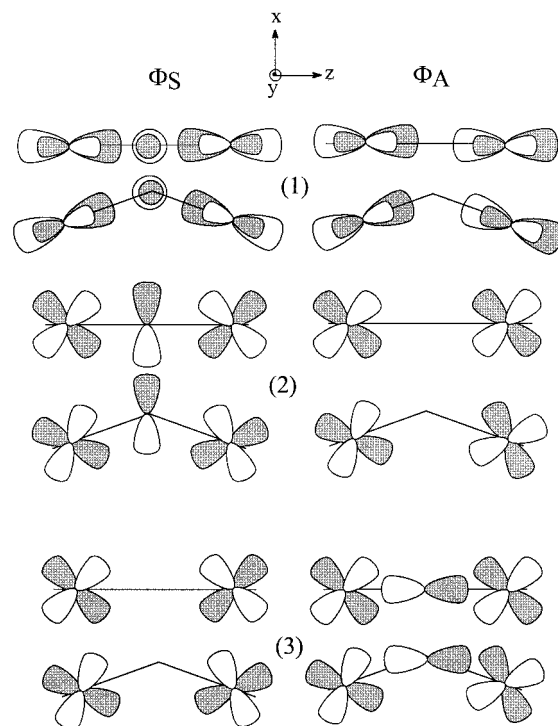
compounds belonging to type I, there is no interdimer AF interaction, or it is extremely weak ($|zJ| < 0.2 \text{ cm}^{-1}$). In the case of compounds exhibiting the type II behavior, the magnitude of the AF exchange is small, and it is accidentally the same as that found in the pentacarboxylate compounds, where it is mediated by the axial carboxylate, i.e., $zJ \cong -2 \text{ cm}^{-1}$. The type III corresponds to a stronger AF interaction ($|zJ| > 10 \text{ cm}^{-1}$).

To account for the existence of these three types of interdimer AF interactions, we have looked for a structural parameter related to the connectivity between dimers and which could be directly correlated to the variations of $|zJ|$ through the whole family. By a thorough examination of all the crystalline structures available for this family of complexes, one geometrical parameter proved to be relevant, i.e., the interdimer angle Ru–Cl–Ru in the complex–anion chains.²⁰ The result of this correlation is presented in Table 6, where we have reported the Ru–Cl–Ru angle and the type of magnetic interaction found in the present work. It should be noted that we have checked in each case that the crystalline structure of the sample studied here was the same as that described in the published crystalline structure. This was achieved by comparison of the experimental powder X-ray diffraction pattern of our sample with the theoretical pattern calculated with the crystalline parameters given in the corresponding publication.²¹

An examination of this table clearly shows that the complexes in which the angle Ru–Cl–Ru is 180° (linear chains) exhibit the strongest interaction (type III behavior); the interdimer exchange decreases with decreasing interdimer angle, and becomes zero for an angle of 125°.

This result can be at least qualitatively explained within the frame of the current theories describing the magnetic exchange through molecular orbital (MO) schemes.^{22,23} Although their respective starting points are quite different, both the Kahn²³ and the Hoffmann²² theories analyze the magnetic exchange as made up of two terms, one antiferromagnetic and one ferromagnetic, the first (AF) increasing with the overlap between the magnetic orbitals. We will interpret qualitatively our experimental correlation following Hoffman's point of view.

The first step in this analysis is thus to construct the symmetric (Φ_S) and antisymmetric (Φ_A) MOs, starting with the

**Figure 4.** Nonzero MO overlaps for the relevant combinations in both the linear and bent configurations of the chloro-carboxylate complexes (see text). (1) p_y (Cl), π^*_{yz} (Ru); (2) p_x (Cl), π^*_{xz} (Ru); (3) p_z (Cl), π^*_{xz} (Ru).**Table 7.** Contributions to the Total Overlap between Neighboring Dimers Arising from the Relevant Combinations of d(Ru) and p(Cl) Atomic Orbitals in Ru₂(RCO₂)₄Cl Compounds

	Φ_S	Φ_A
p_y, π^*_{yz}	$\neq 0$, constant	0
p_x, π^*_{xz}	increases as $\Theta \rightarrow 180^\circ$	0
p_z, π^*_{xz}	0	decreases as $\Theta \rightarrow 180^\circ$

magnetic orbitals of the ruthenium dimers and the chlorine atomic orbitals (AO). The only chlorine AOs having an appropriate energy to interact with the magnetic orbitals of the ruthenium dimers are the 3p AOs. In the Ru₂(RCO₂)₄⁺ moiety, only the π^* antibonding orbital of the metal–metal bond possesses the adequate symmetry to interact with the p(Cl) AO. For the sake of simplicity in the following analysis, we will treat the π^* MO as the 4d_{xz} and 4d_{yz} AO from which they are derived. The second step is to consider the variation of the overlap with the Ru–Cl–Ru angle, for each of the preceding combinations.

These combinations are schematically represented in Figure 4, where the symmetric and antisymmetric combinations of the π^* orbital of two neighboring dimers with the p_x , p_y , and p_z chlorine orbitals are considered, in both linear and bent configurations. We have retained only the configurations that can give rise to nonzero overlap in at least one of these two geometries. Following symmetry considerations, we can see that the π^*_{xz} MO can interact with p_x and p_z AO, and the π^*_{yz} MO gives rise to a nonzero overlap only when combined with the p_y AO. The change in the overlap as a function of the Ru–Cl–Ru angle for each of these six combinations is summarized in Table 7.

The present analysis may be restricted to the comparison between the contributions of Φ_A (p_z, π^*_{xz}) and Φ_S (p_z, π^*_{xz}) to the total overlap, all the other contributions being zero or constant as Θ varies. The contributions of Φ_A (p_z, π^*_{xz}) and

(20) Attempts were made to study the magnetic behavior of two other chloro complexes of this series possessing a 180° interdimer angle: the linear chain forms of the acetato^{17j} and butyrate^{17f} derivatives. However, the crystalline samples that we obtained proved to be a mixture of the linear and the bent (125°) forms; the $\chi(T)$ curves obtained were, consequently, a combination of those corresponding to types I and III.

(21) The simulated powder X-ray diffraction patterns were calculated by E. Amalric (ILL-Grenoble) and J. Laugier (CEA-Grenoble).

(22) Hay, P. J.; Thibeault, J. C.; Hoffmann, R. *J. Am. Chem. Soc.* **1975**, *97*, 4884.

(23) (a) Kahn, O.; Briat, B. *J. Chem. Soc., Faraday Trans. 2* **1976**, *72*, 268. (b) Kahn, O. In *Magneto-Structural Correlations in Exchange Coupled Systems*; Willett, R. D., Gatteschi, D., Kahn, O., Eds.; NATO Asi Series; D. Riedel Publishing Co.: Hingham, MA, 1984; p 37.

Φ_S (p_z , π^*_{xz}) give opposite effects, thus certainly leading to the existence of a minimum in the total overlap for some angle. However, as Θ tends to 180° , the total overlap increases and, consequently, the AF coupling between dimers is expected to increase as the Ru–Cl–Ru angle approaches 180° . This is consistent with the experimental magnetic behavior found for these compounds. Beyond the present qualitative analysis, a quantitative assessment of the different contributions to the total overlap is under way.²⁴

Magnetic Behavior at the Crystal–Liquid Crystal Phase Transition. The first point to be considered in analyzing these results is that the presence of three unpaired electrons per dimer is only a consequence of the lantern-structure of the diruthenium tetracarboxylate unit.^{1b,c} It is thus clear that this binuclear structure is retained in the liquid-crystalline phase for all the complexes studied here. Furthermore, the absence of discontinuity at the crystal–liquid crystal transition temperature (in contrast to that found for divalent ruthenium²⁵ or copper²⁶ carboxylates) suggests that the structural arrangement of the polar cores is essentially retained in the mesophase.²⁷

The study performed in the liquid-crystalline phase of the pentacarboxylate series, $\text{Ru}_2(\text{RCO}_2)_5$, provides a useful piece of information in order to propose a model describing the supramolecular structure in the mesophase. The results described above are an additional support for our proposed structural model of its columnar mesophase,² in which each column is made up of four chains of alternating ...–complex–anion–... units. In such a structure, the magnetic behavior due to the complex–anion interactions within one chain should be similar to that in the crystalline phase, as far as interchain exchange is highly unfavored due to the presence of bulky peripheral hydrocarbon chains.

As far as the mesomorphic phase of the dodecyl sulfate compound, $\text{Ru}_2(\text{O}_2\text{C}-(\text{CH}_2)_{14}-\text{CH}_3)_4\text{DOS}$, as well as those of

the dialkoxybenzoate derivatives $\text{Ru}_2(\text{B}(\text{OC}n)_4\text{Cl}$ and $\text{Ru}_2(\text{B}(\text{OC}n)_5)$, are concerned, one obvious conclusion that can be drawn is that the binuclear structure is retained, as in the case of the pentacarboxylate series. The lack of discontinuity at the transition temperature in the $\chi(T)$ curve may be interpreted as reflecting no (or at least negligible) changes in the coordination sphere of Ru atoms. This evidence will be of interest when new structural information will be available, to propose a structural model for the mesophase of these compounds.

Conclusion

The present magnetic studies provide important information about both the electronic structure of mixed-valent diruthenium carboxylates and the interdimer interactions present in these compounds. They also indicate that no significant structural change occurs at the crystal–liquid crystal transition of these metallomesogens.

The magnetic features of the $\text{Ru}_2(\text{RCO}_2)_4^+$ moiety are essentially independent of the carboxylate substituent R. All the complexes examined in this investigation exhibit g values higher than 2 (with g_\perp greater than g_\parallel), and they all undergo a zero-field splitting of about 70 cm^{-1} . Thus, this high ZFS is a general feature of these compounds, and it must be taken into account in the description of their magnetic behavior.

The present study also shows that some axially coordinated anions can mediate AF interactions between neighboring ruthenium dimers. This interdimer exchange is negligible in the case of dodecyl sulfate anion, and it can reach -1 to -4 cm^{-1} in the case of carboxylate anions. In the chloride series, the magnitude of the interaction was found to be dependent on the angle Ru–Cl–Ru, varying from zero, for an angle of 125° , to less than -10 cm^{-1} for an angle of 180° . A qualitative explanation in terms of MO overlap has been proposed, and a more detailed theoretical work is now under way.

Similar physicochemical studies will be extended to complexes containing different axial ligands, in particular to investigate other properties related to the bridging units between dimers.

Acknowledgment. We thank J. F. Jacquot (CEA/Grenoble) for his valuable assistance in magnetic measurements and more specially for the design and setup of the high-temperature sample environment. We also thank Dr. Pascal Fries (CEA/Grenoble) for providing the refinement program, Dr. Anne-Marie Giroud-Godquin (CEA/Grenoble) for encouraging comments, and Drs. Edith Amalric (Institut Laue-Langevin, Grenoble) and Jean Laugier (CEA/Grenoble) for the simulation of powder X-ray diffraction patterns from crystallographic data.

Supporting Information Available: Elemental analyses, experimental and calculated, collection conditions, crystallographic data, calculated positions of hydrogen atoms, and anisotropic parameters (6 pages). Ordering information is given on any current masterhead page.

IC971366O

- (24) Estiu, G.; Maldivi, P.; Cukiernik, F. D., work in progress.
 (25) (a) Maldivi, P.; Giroud-Godquin, A. M.; Marchon, J. C.; Guillon, D.; Skoulios, A. *Chem. Phys. Lett.* **1989**, *157*, 552. (b) Marchon, J. C.; Maldivi, P.; Giroud-Godquin, A. M.; Guillon, D.; Skoulios, A.; Strommen, D. *Philos. Trans. R. Soc. London* **1990**, *A330*, 109. (c) Bonnet, L.; Cukiernik, F. D.; Maldivi, P.; Giroud-Godquin, A. M.; Marchon, J. C.; Ibn-Elhaj, M.; Guillon, D.; Skoulios, A. *Chem. Mater.* **1994**, *6*, 31.
 (26) Giroud-Godquin, A. M.; Latour, J. M.; Marchon, J. C. *Inorg. Chem.* **1985**, *24*, 4452.
 (27) The small but significant discontinuity in χ at the phase transition temperature found in the $\text{Cu}_2(\text{RCO}_2)_4$ and $\text{Ru}_2(\text{RCO}_2)_4$ series was interpreted^{25,26} as a slight structural rearrangement of the binuclear units in the mesophase, which was also detected by a variety of other experimental techniques.^{25b} Recently, some authors postulated a change from a binuclear to a mononuclear structure at the phase transition for the copper derivatives on the basis of infrared spectroscopic measurements.²⁸ Such a change seems quite difficult to justify for the copper series, on the basis of their observed magnetic behaviour,²⁵ and it can be ruled out also for the diruthenium(II,II) series, in which the presence of two unpaired electrons per dimer is also a consequence of the lantern structure.^{1c}
 (28) Ramos Moita, M. F.; Duarte, M. L. T. S.; Fausto, R. J. *Chem. Soc., Faraday Trans.* **1994**, *90*, 2953.